

The Low-Rank Simplicity Bias in Deep Networks

Minyoung Huh¹ Hossein Mobahi² Richard Zhang³ Brian Cheung^{1,4} Pulkit Agrawal¹ Phillip Isola¹

Abstract

Modern deep neural networks are highly over-parameterized compared to the data on which they are trained, yet they often generalize remarkably well. A flurry of recent work has asked: why do deep networks not overfit to their training data? We investigate the hypothesis that deeper nets are implicitly biased to find lower rank solutions and that these are the solutions that generalize well. We prove for the asymptotic case that the percent volume of low effective-rank solutions increases monotonically as linear neural networks are made deeper. We then show empirically that our claim holds true on finite width models. We further empirically find that a similar result holds for *non-linear* networks: deeper non-linear networks learn a feature space whose kernel has a lower rank. We further demonstrate how linear over-parameterization of deep non-linear models can be used to induce low-rank bias, improving generalization performance without changing the effective model capacity. We evaluate on various model architectures and demonstrate that linearly over-parameterized models outperform existing baselines on image classification tasks, including ImageNet.

1. Introduction

It has become conventional wisdom that the more layers one adds, the better a deep neural network (DNN) performs. This guideline is supported, in part, by theoretical results showing that deeper networks can require far fewer parameters than shallower networks to obtain the same modeling “capacity” (Eldan & Shamir, 2016). While it is not surprising that deeper networks are more expressive than shallower networks, the fact that state-of-the-art deep networks do not overfit, despite being heavily over-parameterized¹, defies classical statistical theory (Geman et al., 1992; Zhang et al., 2017; Belkin et al., 2019).

¹e.g., Dosovitskiy et al. (2020) trains an image classification model that consists of 632 million parameters with 200+ layers on ImageNet (Russakovsky et al., 2015), which only consists of 1.3 million images.

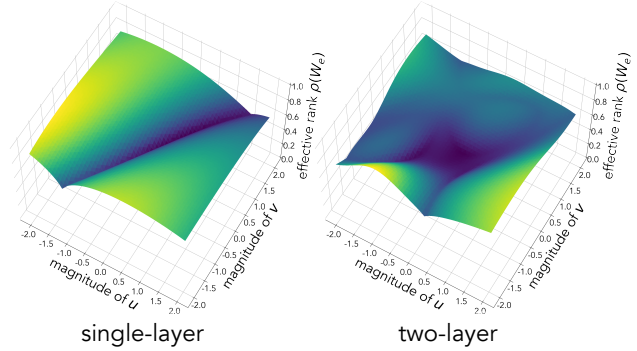


Figure 1. Rank landscape: The landscape of the effective rank ρ of a linear function W_e parameterized either by a single-layer network ($W_e = W$) or a two-layer linear network ($W_e = W_2 W_1$). The visualization illustrates a simplicity bias of depth, where the two-layer model has relatively more parameter volume mapping to lower rank W_e . Both models are initialized to the same end-to-end weights W_e at the origin. Motivated by (Goodfellow et al., 2015), the landscapes are generated using 2 random parameter directions u, v to compute $f(\alpha, \beta) = \rho(W + \alpha \cdot u + \beta \cdot v)$ for the single-layer model and $f(\alpha, \beta) = \rho((W_2 + \alpha \cdot u_2 + \beta \cdot v_2) \cdot (W_1 + \alpha \cdot u_1 + \beta \cdot v_1))$ for the two-layer model ($u = [u_1, u_2]$, $v = [v_1, v_2]$).

In the face of strong empirical results and the absence of clear theoretical guidance, the belief that *over-parameterization via depth improves generalization* is used axiomatically in the design of neural networks. Unlike conventional regularization methods that penalize model complexity (e.g., ℓ_1/ℓ_2 penalty), over-parameterization does not. Yet, like explicit regularization, over-parameterization appears to prevent the model from over-fitting.

Unfortunately, why this *implicit regularization* works is largely unknown. One notable exception is the case of *linear* over-parameterization. To understand this, consider two models, $M_1 : Wx$ and $M_2 : (W_d W_{d-1} \dots W_1)x$. If $W = W_d W_{d-1} \dots W_1$, then these two models are functionally equivalent. However, strangely, when trained using gradient descent, these models find *different* solutions. Namely, the second network finds *lower rank* solutions, despite having d times more parameters. Several explanations of this

Affiliations ¹MIT CSAIL ²Google R. ³Adobe R. ⁴MIT BCS
Correspondence Minyoung Huh - minhuh@mit.edu
Project page minyoungg.github.io/overparam
Code github.com/minyoungg/overparam

phenomenon include over-parameterization acting as momentum in gradient updates (Arora et al., 2018) and nuclear norm bias (Gunasekar et al., 2017; Arora et al., 2019).

Now consider a model $M_3 : W_d\psi(W_{d-1} \dots \psi(W_1(x)))$, where ψ is a non-linear function. In contrast to linear networks, M_3 is more “expressive” and cannot, in general, be represented by linear models M_1, M_2 . With the increase in modeling capacity, one might expect the deeper non-linear network to find more complex solutions. On the contrary, and quite intriguingly, we show that even for **non-linear networks, an increase in depth leads to lower rank (i.e., simpler) embeddings**. This is in alignment with the work from Valle-Perez et al. (2019), which argues that deep networks have a simplicity bias — the parameters of the network map to simple functions. We extend this theory to show that **depth increases the volume of low-rank solutions** in the parameter space (see Figure 1), and we conjecture that this makes deeper networks more likely, by chance, to find low-rank solutions. Our work thereby expands the growing body of work on over-parameterization and highlights the central role of depth in finding solutions with lower rank weights for both linear and non-linear networks. We further use this theory to demonstrate how one can use “depth” as a practical regularizer, achieving better generalization performance on CIFAR (Krizhevsky et al., 2009) and ImageNet (Russakovsky et al., 2015), using widely adopted architectures such as AlexNet (Krizhevsky et al., 2017) and ResNets (He et al., 2016). We achieve this by linear over-parameterization of individual layers of a non-linear model (Section 6.2).

2. Related works

Linear networks Linear networks have been used in lieu of non-linear networks for analyzing the generalization capabilities of deep networks. These networks have been widely used for analyzing learning dynamics (Saxe et al., 2014) and forming generalization bounds (Advani et al., 2020). Notable work from Arora et al. (2018) shows that over-parameterization induces training acceleration and that the effects of over-parameterization cannot be approximated by an explicit regularizer. Furthermore, Gunasekar et al. (2017) shows that linear models with gradient descent converge to a minimum nuclear norm solution on matrix factorization problems. Although mainly used for simplifying theory, Bell-Klijger et al. (2019) demonstrate the practical applications of deep linear networks.

Low-rank biases of linear networks Multi-layered linear neural networks have been known to be biased towards low-rank solutions. One of the most widely studied regime is on matrix factorization with gradient descent under isometric assumptions (Tu et al., 2016; Ma et al., 2018; Li et al., 2018). This phenomenon is further analyzed on least-squares re-

gression by Gidel et al. (2019). One of the most relevant works to ours is Arora et al. (2019) that shows that matrix factorization tends to low nuclear-norm solutions with singular values decaying faster in deeper networks. In a similar light, Pennington et al. (2018) shows that the input-output Jacobian’s spectral distribution is determined by depth.

Simplicity bias of neural networks Recent works have indicated that neural networks tend to find simple solutions. For example, linear models trained with gradient descent have been shown to find max-margin solutions (Soudry et al., 2018; Nacson et al., 2019; Gunasekar et al., 2018). Separately, in the perspective of algorithmic information theory, Valle-Perez et al. (2019) demonstrated that deep networks have simplicity bias where most random points in the parameter space map to low-complexity functions. Furthermore, Nakkiran et al. (2019) and Arpit et al. (2017) have shown that networks learn in stages of increasing complexity. Whether these aspects of simplicity bias are good or bad has been studied (Shah et al., 2020).

Complexity measures for neural networks In parallel, a growing number of works indicate that the matrix norm is not a good measure for characterizing neural networks. Shah et al. (2018) shows that minimum norm solution is not guaranteed to generalize well. These findings are echoed by Razin & Cohen (2020), which demonstrate that implicit regularization of matrix factorization cannot be characterized by norms and proposes rank as an alternative measure.

Biases in non-linear networks For non-linear networks, understanding the biases has been mostly empirical, with the common theme that over-parameterization of depth or width improves generalization performance (Neyshabur et al., 2015; Nichani et al., 2020; Golubeva et al., 2021; Hestness et al., 2017; Kaplan et al., 2020) but also leads to networks that are capable of over-fitting to random labarpit2017closerels (Zhang et al., 2017). Recently, a few works have mixed linear layers into non-linear networks, such as rank-minimizing auto-encoders (Jing et al., 2020) and compressing classification models (Guo et al., 2020).

3. Preliminaries

In this section, we discuss notations for linear networks and over-parameterization.

3.1. Linear neural networks

Simple linear network A simple linear neural network transforms input $x \in \mathbb{R}^{n \times 1}$ to output $\hat{y} \in \mathbb{R}^{m \times 1}$, with a learnable parameter matrix $W \in \mathbb{R}^{m \times n}$,

$$\hat{y} = Wx. \quad (1)$$

For notational convenience, we omit the bias term.

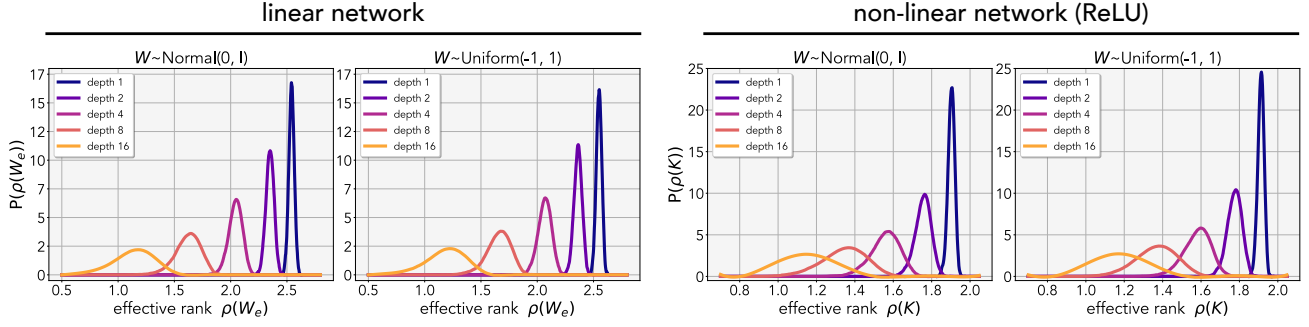


Figure 2. Deep networks are biased toward low-rank: The approximated probability density function (PDF) of the effective rank ρ over the parameter set \mathcal{W} (left) and kernels computed from non-linear ReLU networks (right). For linear networks, the weights are drawn from a random distribution and the PDF is computed on the end-to-end matrix W_e . To infer the rank of a non-linear networks, we measure the effective rank on the feature kernel matrices (See Section 5.1). The kernel matrix is computed with 256 random inputs, and we use 4096 parameter samples for both linear and non-linear networks to approximate the cumulative distribution function which is then used to compute the PDF via finite difference. We apply Savitzky–Golay filter (Savitzky & Golay, 1964) on the approximation to smoothen out the noise. We observed there exists more probability mass for lower-rank rank solutions when adding more layers. The experiment is repeated for both normal and uniform distributions.

Over-parameterized linear network One can over-parameterize a linear neural network by defining d matrices $\{W_i\}_{i=1}^d$ and multiplying them successively with input x :

$$\hat{y} = W_d W_{d-1} \cdots W_1 x = W_e x, \quad (2)$$

where $W_e = \prod_{i=1}^d W_i$. As long as the matrices are of the correct dimensionality — matrix W_d has m columns, W_1 has n rows, and all intermediate dimensions $\{\dim(W_i)\}_{i=2}^{d-1} \geq \min(m, n)$ — then this over-parameterization expresses the same set of functions as a single-layer network.

We disambiguate between the collapsed and expanded set of weights by referring to $\{W_i\}$ as the over-parameterized weights and W_e as the end-to-end or the effective weights.

4. The inductive bias of depth

What are the implications of searching for solutions in $\{W_i\}$ versus directly in W_e ? One difference is that the gradient direction $\nabla_{\{W_i\}} \mathcal{L}(\{W_i\})$ is usually different than $\nabla_{W_e} \mathcal{L}(W_e)$ for a typical loss function \mathcal{L} (see Appendix E). The consequences of this difference have been previously studied in Arora et al. (2018; 2019), where the over-parameterized update rule has been shown to accelerate training and encourage singular values to decay faster, resulting in a low nuclear-norm solution. Here we motivate a similar result from a different perspective: random settings of $\{W_i\}$ are biased to correspond to low-rank effective matrix W_e .

In practice, it is difficult for a matrix to be strictly rank-deficient due to numerical fluctuations. Furthermore, we would like to characterize weights with small normalized singular values as “lower rank” than those which do not.

Therefore, to make meaningful comparisons of rank, we first require a non-strict measure for approximating the rank of weight matrices. In our work, we mainly consider the pseudo-rank measure known as effective rank.

Definition 1 (Effective rank). (Roy & Vetterli, 2007) For any matrix $A \in \mathbb{R}^{m \times n}$, the effective rank ρ is defined as the Shannon entropy of the normalized singular values:

$$\rho(A) = - \sum_{i=1}^{\min(n,m)} \bar{\sigma}_i \log(\bar{\sigma}_i),$$

where $\bar{\sigma}_i = \sigma_i / \sum_j \sigma_j$ are normalized singular values, such that $\sum_i \bar{\sigma}_i = 1$. This is also known as the spectral entropy.

This measure gives us a meaningful representation of “continuous rank”, which is maximized when the magnitude of the singular values are all equal and minimized when a single singular value dominates relative to others. The effective rank provides us with a metric that indicates the relative ratio of the singular values: a summarization of the distribution envelope. Contrary to prior work, which refers to low nuclear norm solutions as low-rank solutions (Arora et al., 2019), we did not find nuclear norm to be a meaningful metric for neural networks in practice. This is because the nuclear norm is an unnormalized measure that can be arbitrarily scaled. The comparison of various common pseudo-metrics of rank is reported in the Appendix A.

4.1. Low-rank bias of deep linear networks

To show that deep linear models are biased toward low-rank, we prove that the effective rank of the model monotonically decreases as we increase the number of layers.

A simple intuition can be derived from the fact that the product of matrices can only decrease the rank of the resulting matrix: $\text{rank}(AB) \leq \min(\text{rank}(A), \text{rank}(B))$ (Friedberg et al., 2003). To prove a similar inequality for the effective rank, we take inspirations from works from random matrix theory studying the spectral distribution under matrix multiplications (Akemann et al., 2013a,b; Burda et al., 2010). We leverage the results from (Pennington et al., 2017; Neuschel, 2014) to show the following:

Theorem 1. *Let ρ be the effective rank measure defined in Definition 1. For a linear neural network with d -layers, where the parameters are drawn from the same Normal distribution $\{W_i\}_{i=1}^d \sim \mathcal{W}$, the effective rank of the weights monotonically decreases when increasing the number of layers when $\dim(W) \rightarrow \infty$,*

$$\rho(W_d W_{d-1} \dots W_1) \leq \rho(W_{d-1} \dots W_1)$$

Proof. See Appendix D.

Intuitively, if any constituent matrices are low-rank, then the product of matrices will also be low-rank. We directly quantify this property by measuring the density of the effective rank as a function of the number of layers in the over-parameterized linear network. We randomly initialize the network's weight matrices, using uniform $W_i \sim \mathcal{U}(-1, 1)$ or Normal distributions $W_i \sim \mathcal{N}(\mathbf{0}, \mathbf{I})$. Initializing the model with a uniform distribution implies that every point in the weight hyper-cube is equally probable. For this empirical study, we use input, output, and intermediate dimensions of 16, giving parameters $\{W_i\} \in \mathbb{R}^{d \times 16 \times 16}$ for a network with d layers. We draw 4096 random parameter samples and compute the effective rank on the resulting end-to-end matrix. In Figure 2, we see the density of the distribution shifts towards the left (lower effective rank) when increasing the number of layers. These distributions have a reasonably small overlap and smoothen out with increased depth. Our observations indicate that depth alters the parameter geometry, increasing the likelihood of observing low-rank parameters in deeper networks. These results suggest the following conjecture:

Conjecture 1. *The deeper the net, the greater the proportion of parameter space that maps to low-rank functions; hence, deeper models are more likely to converge to low-rank functions by chance.*

4.2. Characterizing rank of non-linear networks

Contrary to linear networks, non-linear networks gain capacity when adding more layers — the sets of functions they can approximate (Eldan & Shamir, 2016) are no longer equivalent. While we cannot directly compare the weights, we can compare the embedding space induced by non-linear

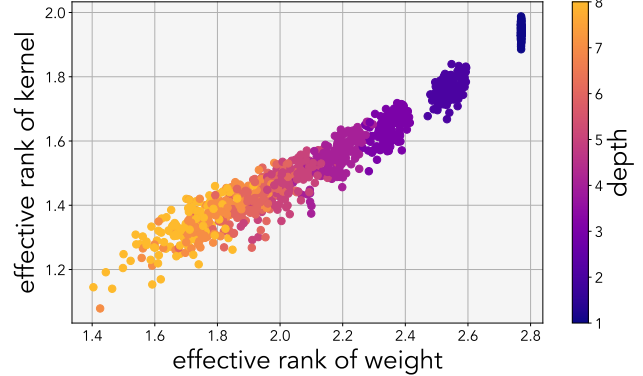


Figure 3. Relationship between kernel-rank and weight-rank: Each point represents randomly drawn network weights. For each sample, we compute the rank on the effective weight and also the linear kernel. The kernel is constructed from 256 randomly drawn vectorized MNIST images and the weights are initialized using Normal distribution. We repeat this procedure 128 times per depth for a total of 1024 samples. The rank of the kernel and the rank of the weight have a linear relationship.

networks. By representing the outputs of a neural network as a kernel matrix (Kriegeskorte et al., 2008; Jacot et al., 2018), we can compute the “rank” of the network with respect to the dataset *on the output-space*.

The intuition on measuring the rank on the output-space of the network becomes clearer in linear networks, where the rank of the outputs is maximally spanned by the rank of the weights in the network. For some weight matrix $W \in \mathbb{R}^{m \times n}$ and input data $X \in \mathbb{R}^{n \times p}$ with p -samples, WX is the output representation of the network. Then, the $\text{rank}(W) = \text{rank}(WX)$ when X is full-rank. Since the dimensionality of WX changes across models with different architectures, we analyze the rank on the kernel constructed from these features. A linear kernel constructed from d -layer linear network is defined as $K_d = (W_{d:1}X)^T (W_{d:1}X)$, where $\text{rank}(K_d)$ depends on $\text{rank}(W_{d:1})$. It follows that analyzing the rank of the output provides an alternative way to measure the relationship between neural networks and rank — where the dimensionality of the embedded points (i.e., the rank of the kernel) is related to the rank of the function that produced them.

We show in Figure 3 that, empirically, there is indeed a tight relationship between weight rank and kernel rank, plotting this relationship for random deep linear networks applied to random subsets of the MNIST dataset. The figure shows a linear relationship between the rank of the weight matrix and the rank of the kernel. Moreover, it becomes apparent that the number of layers dictates the rank of the underlying function parameterized by the network.

Now, using our kernel rank measure, we can test our conjecture that *deeper non-linear models converge to low-rank solutions simply due to the abundance of parameters that*

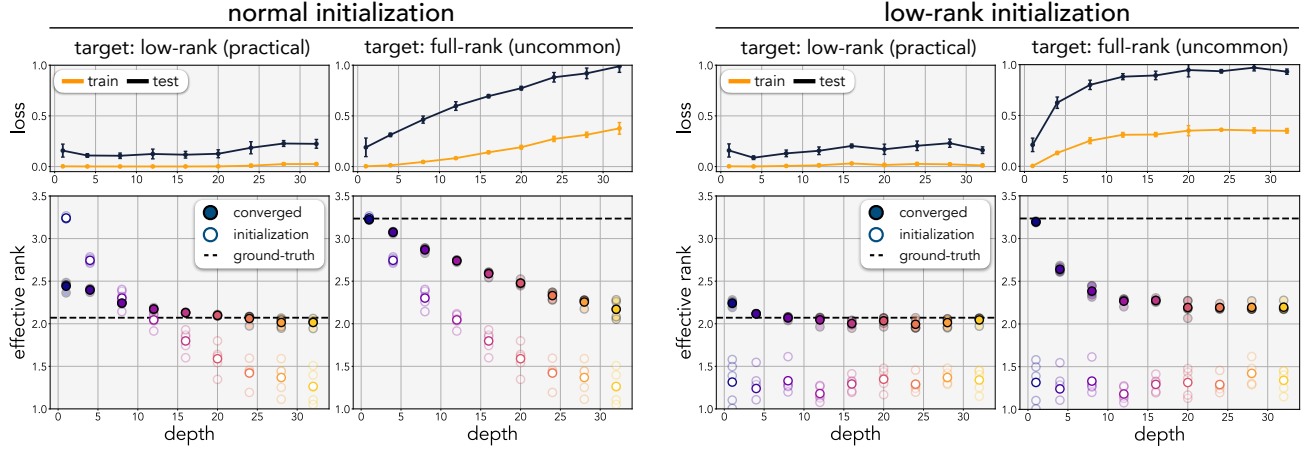


Figure 4. Bias of parameterization: Visualization of the effective rank from initialization to convergence on various depths. For each depth we train linear networks using gradient descent on a toy least squares regression problem where we know the rank of the solution. We repeat our experiments 5 times with different seeds (transparent dots) and we report the median of these runs. The rank at initialization and convergence is indicated with white and colored dots respectively. We use Kaiming initialization (He et al., 2016) for the weights — a scaled normal distribution. Since the product of normally distributed weights are no longer normally distributed, the effective-rank becomes lower even at initialization. On the right, we demonstrate that this low-rank bias is from the parameterization and not from initialization by repeating the experiments with weights being drawn from the same distribution as the 32-layer model.

get mapped to low-rank functions. We run a similar experiment as we did for linear networks in Figure 2 (left). We approximate the PDF of effective rank over the kernels computed from randomly sampled deep non-linear networks. We sample the weights in the same manner as for deep linear networks, and for each sampled network, we construct a kernel using 256 randomly drawn input samples. We repeat this 4096 times to approximate the underlying distribution. In Figure 2 (right), we compute the PDF on the effective rank of these kernels and find a strikingly similar distribution as observed in linear networks, reaffirming our conjecture that these biases also exist in non-linear networks.

The remainder of the paper focuses on empirical studies to show that while effective weights of linear models are more likely to be low-rank, so are the solutions found under the regime of first-order gradient optimization for both linear and non-linear models.

5. Experiments on least-squares

To demonstrate that our conjecture holds, we show on least-squares that deeper models tend to converge towards low-rank weights. We then show that similar observations can be seen in non-linear networks when treating the model as a non-linear projection and measuring the rank of the kernels constructed from the output features.

5.1. Least-squares with neural-networks

As a motivation, consider a least-squares problem where we know the rank of the solution. The set of example pairs

$(x, y) \in \mathcal{X}, \mathcal{Y}$ are generated from the low-rank weights W^* , and the goal is to regress a parameterized function $f_W(\cdot)$ to minimize the squared-distance $\|f_W(x) - y\|_2^2$. By construction, the rank(W^*) is denoted as the *task rank* or, informally stated, the intrinsic dimensionality of the data. For our experiments, the number of training examples is strictly fewer than the number of model parameters. The problem then becomes under-determined, ensuring that there exists more than one minimizing solution.

Linear neural network For our toy problem, we optimize a single-layer network $W \in \mathbb{R}^{32 \times 32}$ where the task-rank is set to 8. All models are trained until the training loss reaches zero. In Figure 4, we show that optimizing over single-layer networks results in a solution that has a higher effective rank than the ground-truth. Further increasing the number of layers decreases the effective rank of the converged weights, where the distribution of the singular values becomes more concentrated towards the top singular values. Even when all the models have the same training loss, the test-loss varies across models — with the test loss being minimized when the effective rank approximately aligns with the ground truth rank of the dataset. We repeat these experiments where the underlying weights are full-rank. In this case, we observed that deeper models could not converge to the ground-truth rank nor find a minimizing solution.

As our observation shows, rank is a function of depth, and it monotonically decreases as more layers are added. The model achieves its best generalization performance when the effective rank of the end-to-end weight matrix approximately aligns with the ground-truth task rank (the dotted

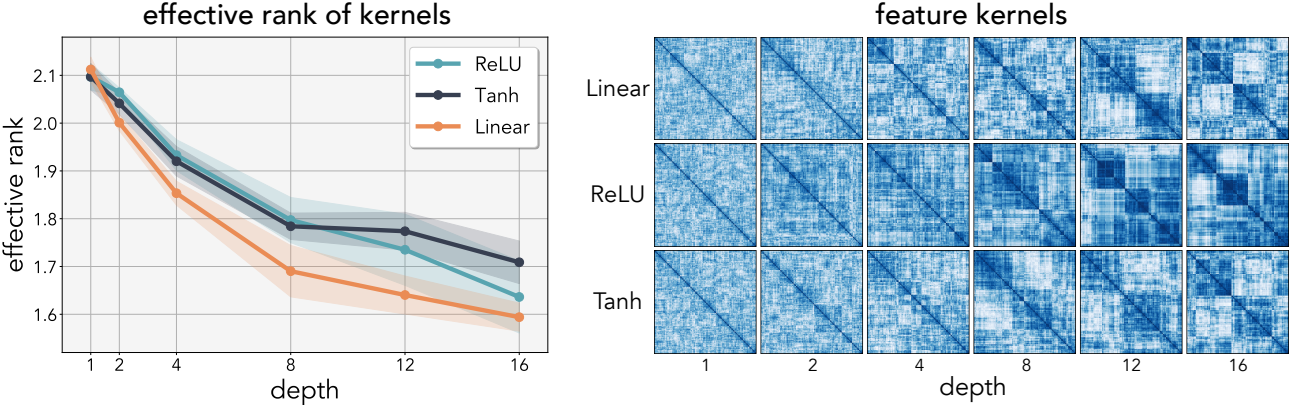


Figure 5. Kernel analysis of networks: Kernel-matrices are computed using the cosine-distance on the features of the test-set after achieving zero-training loss. The effective rank is computed on the kernels for both linear and non-linear model with rectified (ReLU) and logistic (Tanh) non-linearities. Increasing the number of layers decreases the effective rank of the kernel. We further hierarchically cluster (Rokach & Maimon, 2005) the kernels and visualize them on the right. We observed emergence of block structures in the kernels as we increase the number of layers, indicating the output mapping becomes more low-rank with depth.

line), and further increasing the depth only hurts performance. Although conventional wisdom states that adding more layers should always help, *our observations indicate there is a sweet spot of depth*, where the model is not too deep and not too shallow, and this sweet spot depends on the true complexity of the data.

Non-linear neural network

To analyze non-linear networks we construct a kernel matrix of dimension $K \in \mathbb{R}^{p \times p}$ where p is the size of the test set, and the ij -th entry corresponds to some distance kernel $K_{ij} = \kappa(\phi_i, \phi_j)$. We use the model’s intermediate features ϕ before the linear classifier and use cosine distance for the distance kernel, a common method for measuring distances in feature space (Kiros et al., 2015; Zhang et al., 2018). Since the dimensionality of the kernel depends on the dataset size and not the model architecture, it enables comparison across different model topologies when the test-loss is equivalent.

In our test scenario, all models converge to zero training error, enabling fair comparison across networks of various depths. In Figure 5, we visualize the results using the same least-squares setup, where we interleave a ReLU for every fully-connected layer we add. We observed that kernels constructed from both linear and non-linear models are lower-rank when increasing the number of layers. This observation is also visually indicated on Figure 5 (right) with the emergence of the block-structures in the hierarchically clustered kernels (Rokach & Maimon, 2005). This experiment demonstrates that deeper non-linear networks converge to solutions with lower rank kernels.

6. Over-parameterization of non-linear networks as an implicit regularizer

Low-rank approximation has served as a central tool for analyzing the underlying structure of linear systems, providing means for finding the simplest approximation to a complex and noisy system (i.e., matrix completion, collaborative filtering, PCA). As famously noted by Solomonoff (1964)’s theory of inductive inference, the simplest solution is often the best solution, suggesting that low-rank parameters in neural networks could improve generalization and robustness to overfitting. Ample evidence from prior works (Szegedy et al., 2015; He et al., 2016) suggests that over-parameterization of non-linear models improves generalization on a fixed dataset. However, increasing the number of non-linear layers also increases the modeling capacity, thereby making it difficult to isolate the effect of depth.

Nevertheless, since a non-linear network is composed of many linear components, such as fully connected and convolutional layers, we can over-parameterize these linear layers to induce a low-rank bias in the weights without increasing the modeling capacity. We observe that such linear over-parameterization improves generalization performance on classification tasks. Furthermore, we find that such implicit regularization outperforms models trained with several choices of explicit regularization.

6.1. Expanding a non-linear network

A deep non-linear neural network with l layers is parameterized by a set of l weights $W = \{W_1, \dots, W_l\}$. The output of the j -th layer is defined as $\phi_j = \psi(f_{W_j}(\phi_{j-1}))$, for some non-linear function ψ and input feature ϕ_{j-1} . The

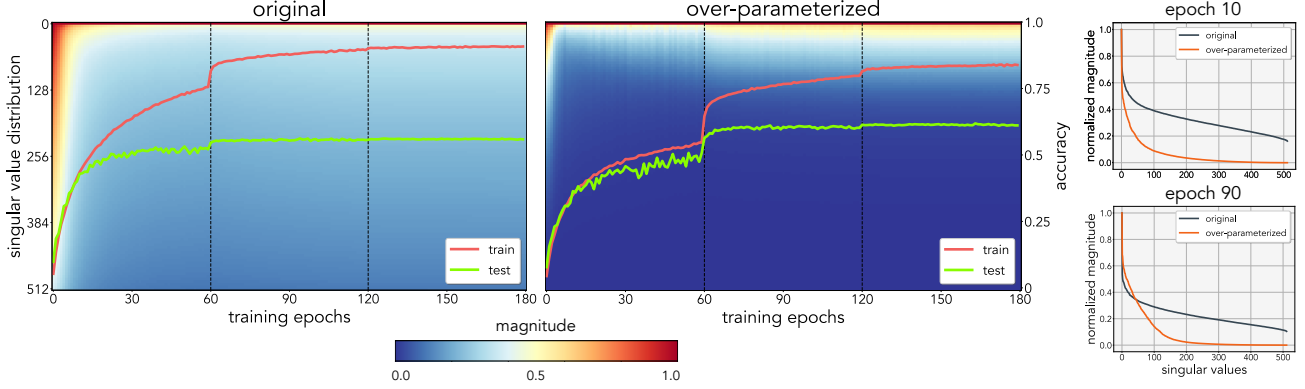


Figure 6. Spectral dynamics: Singular values of the CNN’s `conv-4` weights for both original (left) and linearly over-parameterized (right) model throughout training. The model is over-parameterized by a factor of 4. Singular values of the convolutional weights are computed by adopting an approximate method in (Yoshida & Miyato, 2017). These models were trained on CIFAR100 using SGD. The dotted lines (—) indicate the learning step schedule, and train and test losses are overlayed on top of the distribution. On the right, we visualize the corresponding singular values at epoch 10 and 90. The over-parameterized model exhibit less overfitting, with lower training accuracy and higher testing accuracy.

initial feature map is the input $\phi_0 = x$, and the output is the final feature map $y = \phi_l$. We can expand a model by depth d by expanding all linear layers, i.e. redefining $f_{W_j} \rightarrow f_{W_j^d} \circ \dots \circ f_{W_j^1} \forall j \in \{1, \dots, l\}$. We illustrate this in Figure 7. We describe this operation for fully connected and convolutional layers.

Fully-connected layer A fully-connected layer is parameterized by weight $W \in \mathbb{R}^{m \times n}$. One can over-parameterize W as a series of linear operators defined as $\prod_{i=1}^d W_i$. For example, when $d = 2$, $W \rightarrow W_2 W_1$, where $W_2 \in \mathbb{R}^{m \times h}$ and $W_1 \in \mathbb{R}^{h \times n}$ for some hidden dimension h . The variable h is referred to as the width of the expansion and can be arbitrarily chosen. In our experiments, we choose $h = n$ unless stated otherwise. Note that $h < \min(m, n)$ would result in a rank bottleneck and explicitly reduce the underlying rank of the network.

Convolutional layer A convolutional layer is parameterized by weight $W \in \mathbb{R}^{m \times n \times k \times k}$, where m and n are the output and input channels, respectively, and k is the dimensionality of the convolution kernel. For convenience, we over-parameterize by adding 1×1 convolution operations. $W_d * W_{d-1} * \dots * W_1$, where $W_d \in \mathbb{R}^{m \times h \times 1 \times 1}$, $W_{d-1}, \dots, W_2 \in \mathbb{R}^{h \times h \times 1 \times 1}$ and $W_1 \in \mathbb{R}^{h \times n \times k \times k}$. Analogous to the fully-connected layer, we choose $h = n$ to avoid rank bottleneck.

The work by Golubeva et al. (2021) explores the impact of width h . Similar to their findings, we observed using the larger expansion width of to slightly improve performance. We use $h = 2n$ for our ImageNet experiments.

6.2. Image classification with over-parameterization

Using the aforementioned expansion rules, we over-parameterize various architectures and evaluate on a suite of standard image classification datasets: CIFAR10, CIFAR100, ImageNet. All models are trained using SGD with a momentum of 0.9. For data-augmentation, we apply a random horizontal flip and random-resized crop. We follow standard training procedures² and only modify the network architecture.

In Figure 6, we compare a CNN trained without (left) and with (right) our over-parameterization (expansion factor $d = 4$) on CIFAR100. The CNN consists of 4 convolutional layers and 2 fully connected layers; the architecture details are in Appendix B. We overlay the dynamics of the singular values of the `conv-4` layer throughout training (our observations are consistent across all other layers). The spectral distribution is normalized by the largest singular value and are sorted in descending order $\sigma_i(A) \geq \sigma_{i+1}(A)$ for $i < 1 \leq \min(m, n)$. Similar to linear networks, we observe that the individual weights of the over-parameterized model become biased towards low-rank weights. Both original and linearly over-parameterized models exhibit a rank contracting behavior throughout training, but unlike the original, the majority of the singular values of the over-parameterized model are close to zero. In addition, we observe that the rank initially increases in the first couple of iterations and then significantly dips before bouncing back and converging to a steady-state rank. We found this phenomenon to be consistent across optimizers, normalization layers, and initializations.

²<https://github.com/pytorch/examples/blob/master/imagenet>

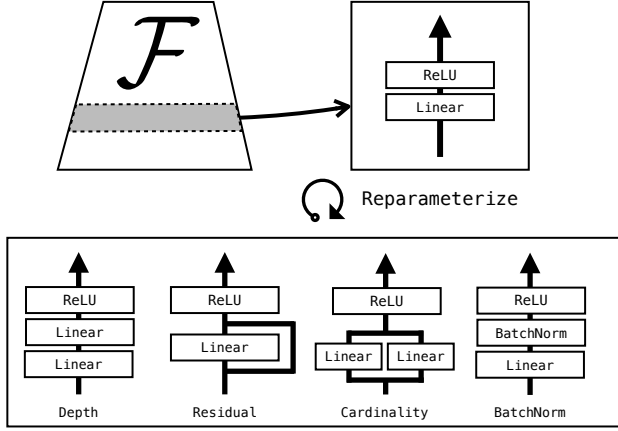


Figure 7. Linear reparameterization: For a model \mathcal{F} , we can reparameterize any linear layer to another functionally equivalent layer (shown in the box below). In this work we mainly explore reparameterization of depth. Batch-norm and any other running-statistics driven normalization layers are linear only at test time.

We further quantify the gain in performance from linear over-parameterization in Table 1. The learning rate is tuned per configuration, and we report the best test accuracy throughout the training. We try various over-parameterization configurations and find an expansion factor of 4 to be the sweet spot, with a gain of +6.3 for CIFAR100 and +2.8 for CIFAR10. The optimal expansion factor depends on the depth of the original network, and in general, we observe a consistent improvement for over-parameterizing models with < 20 layers on image classification.

We scale up our experiments to ImageNet, a large-scale dataset consisting of 1.3 million images with 1000 classes, and show that our findings hold in practical settings. For these experiments, we use standardized architectures: AlexNet (Krizhevsky et al., 2012) which consists of 8-layers, and ResNet10 / ResNet18 (He et al., 2016) which consists of 10 and 18 layers, respectively. If our prior observations hold true, we would expect the gain in performance from over-parameterization to be reduced for deeper models. This is, in fact, what we observed in Table 2, with moderate gains in AlexNet and less for ResNet10 and even less for ResNet18. In fact, starting from ResNet34, we observe linearly over-parameterized models perform worse than the original. These experiments fortify our claims that adding too many layers can over-penalize the weights of the model.

To find out whether the advantages of over-parameterization can be approximated by explicit regularizers, we directly compare the performance in Table 3 on CIFAR. These regularizers include popular ℓ_1 and ℓ_2 norm-based regularizers and commonly-used pseudo-measures of rank. These pseudo-measures of rank, such as effective-rank and nuclear-norm, require one to compute the singular value decompo-

Factor	Expansion			CIFAR10		CIFAR100	
	FC	Conv	accuracy	gain \uparrow	accuracy	gain \uparrow	
1x	-	-	86.9	-	57.0	-	
2x	✓	-	87.1	+0.2	58.4	+1.4	
2x	-	✓	87.8	+0.9	61.0	+4.0	
2x	✓	✓	89.1	+2.2	61.2	+4.2	
4x	✓	-	87.3	+0.4	59.7	+2.7	
4x	-	✓	89.1	+2.2	61.3	+4.3	
4x	✓	✓	89.0	+2.1	63.5	+6.5	
8x	✓	-	85.9	-1.0	58.8	+1.8	
8x	-	✓	88.5	+1.6	61.6	+4.6	
8x	✓	✓	88.0	+1.1	61.5	+4.5	

Table 1. Over-parameterization ablations: A nonlinear CNN with 4 convolution and 2 linear layers trained on CIFAR10 and CIFAR100 with various degrees of linear over-parameterization.

architecture	ImageNet		
	original	over-param	gain \uparrow
AlexNet (2x)	57.3	59.1	+1.8
ResNet10 (2x)	62.8	63.7	+0.9
ResNet18 (2x)	67.3	67.7	+0.4

Table 2. ImageNet: We show on existing architectures, that linear over-parameterization can improve generalization performance. The benefit plateaus off when using deeper models. We did not see a noticeable improvement starting from ResNet34. ResNets were trained using.

sition, which is computationally infeasible on large-scale models. We observe over-parameterization to marginally out-perform explicit regularizers, including rank penalties. Moreover, combining norm-based regularizers with over-parameterization further improves performance. Even if rank-measures are effective ways of characterizing the models, explicitly regularizing for these metrics did not help. This may be explained by the fact that regularizers are inherently different than over-parameterization (Arora et al., 2018). For example, a model trained with a regularizer will have a non-zero gradient, even at zero training loss, while the over-parameterized model will not. Another potential reason is that one needs to jointly consider the bias induced in the parameter-space and also the learning dynamics.

6.3. Bias of parameterization or initialization?

When linearly over-parameterizing our models, we initialize our weights using Kaiming initialization (He et al., 2016), a popular variant of the Normal initialization that bounds the variance of the weights. Using such an initialization method allows us to enforce models that are over-parameterized to have the same output variance, regardless of the depth factor. We find this to be critical for stabilizing our training.

Although using such initialization preserves the variance, over-parameterization changes the underlying distribution of

regularization	CIFAR10		CIFAR100	
	accuracy	gain \uparrow	accuracy	gain \uparrow
none (baseline)	86.9	-	57.0	-
low-rank initialization	86.8	-0.1	57.2	+0.2
ℓ_2 norm	87.2	+0.3	57.0	+0.0
ℓ_1 norm	87.4	+0.5	60.0	+3.0
nuclear norm	87.0	+0.1	58.1	+1.1
effective rank	86.9	+0.0	57.2	+0.2
stable rank	87.6	+0.9	58.3	+1.3
frobenius ² norm	87.0	+0.1	59.2	+2.2
over-param (2x)	89.1	+2.2	61.2	+4.2
over-param (2x) + ℓ_2	89.6	+2.7	61.1	+4.1
over-param (2x) + ℓ_1	89.7	+2.8	63.3	+6.3

Table 3. **Explicit regularizers:** We compare models trained with various weight regularizers. Over-parameterization consistently outperform explicit regularizers.

the effective weights. That is, even if the individual weights are normally distributed, the effective weights constructed from a series of matrix multiplications result in a distribution that has a very high density around zero. For the product 2 weights, this becomes a symmetric χ -squared distribution, with 1 degrees of freedom. Hence, it is possible that our observations could simply stem from the initialization bias.

In Table 3, we show that initializing the model using the same distribution (“low-rank initialization”) from the over-parameterized model performs comparably to the model that was trained from the Normal distribution. Furthermore, in Figure 4 (right), we repeat our linear network experiments by initializing all the networks to the distribution associated with the 32-layer model. We found the bias of the parameterization, not the initialization, to be the main contributing factor for the low-rank bias.

6.4. Extension to residual connections

In this work, we concentrate our analysis on the depth and its role in both linear and non-linear networks. Yet, the ingredients that make up what we know as state-of-the-art models today are more than just depth. From cardinality (Xie et al., 2017) to normalization (Ioffe & Szegedy, 2015) and residual connections (He et al., 2016), numerous facets of parameterization have become a fundamental recipe for a successful model (see Figure 7). Of these, residual connections have the closest relevance to our work.

What is it about residual connections that allow the model to scale arbitrarily in depth, while vanilla feed-forward networks cannot? One possibility is that beyond a certain depth, the rank of the solution space reduces so much that good solutions no longer exist. In other words, the implicit rank-regularization of depth may take priority over the fit to training data. Residual connections are essentially “skip connections” that can be expressed as $W \rightarrow W + \mathbf{I}$, where \mathbf{I}

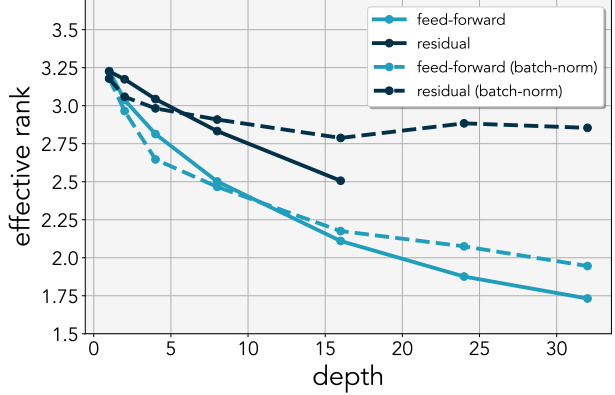


Figure 8. **Residual connections:** The effective rank of linear models trained with and without residual connection on a low-rank least-squares problem. Contrary to feed-forward networks, residual networks maintains the effective rank of the weights even when adding more layers. Residual networks without batch-normalization suffer from unstable output variance after 16 layers.

is the identity matrix (Dirac tensor for convolutions). There are two interpretations of what these connections do: one is that identity preservation prevents the rank-collapse of the solution space. The other interpretation is that residual connections reduce the *effective depth* — the number of linear operators from the input to the output (e.g., ResNet50 and ResNet101 have the same effective depth), which prevents rank-collapse of the solution space. Results in Figure 8 confirm this intuition. ResNets, unlike linear networks, *do not* exhibit a monotonic rank contracting behavior and the effective rank plateaus after 8 layers, regardless of using batch-normalization or not. Furthermore, preliminary experiments on least-squares using linear residual networks indicate that the effective rank of the solution space is also bounded by the number of layers in the shortest and longest path from the inputs to the outputs. A thorough study on the relationship between residual connections and rank is left for future work.

7. Discussion

We conclude by discussing several implications of our work:

Parameterization matters One of the main ingredients in any machine learning algorithm is the choice of hypothesis space: what is the set of functions under consideration for fitting the data? Although this is a critical choice, *how the hypothesis space is also parameterized matters*. Even if two models span the same hypothesis space, the way we parameterize the hypothesis space can ultimately determine which solution the model will converge to — recent work has shown that networks with the better neural reparameterizations can find more effective solutions (Hoyer et al., 2019). The automation of finding the right parameterization

also has a relationship to neural architecture search (Zoph & Le, 2017), but architecture search typically conflates the search for better hypothesis spaces with the search for better parameterizations of given hypothesis space. In this work, we have explored just one way of reparameterizing neural nets – stacking linear layers – which does not change the hypothesis space, but many other options exist (see Figure 7). Understanding the biases induced by these reparameterizations may yield benefits in model analysis and architectural designs.

Deep over-parameterization vs. regularization We have argued that depth acts as an inductive bias toward simple (low-rank) solutions because the relative volume of simple solutions in deeper parameter space is larger, extending prior arguments by Valle-Perez et al. (2019). This effect is qualitatively different than explicit regularization in that it does not change the objective being minimized. Occam’s razor states that the best solution is the simplest that fits the data (as has been formalized in various notions of optimal inference (Solomonoff, 1964)). Too strong an explicit regularizer can prefer simple solutions that do not fit the data, which is incorrect when the true solution is, in fact, complex. Picking a parameterization in which simple solutions are more prevalent but not enforced is an alternative way to approximate the idea of Occam’s razor. Our experiments, which show that explicit rank regularization underperforms compared to deep over-parameterization, suggest that this implicit regularization may have advantages.

Acknowledgements

We would like to thank Anurag Ajay, Lucy Chai, Tongzhou Wang, and Yen-Chen Lin for reading over the manuscript and Jeffrey Pennington and Alexei A. Efros for fruitful discussions. Minyoung Huh is funded by DARPA Machine Common Sense and MIT STL. Brian Cheung is funded by an MIT BCS Fellowship.

This research was also partly sponsored by the United States Air Force Research Laboratory and the United States Air Force Artificial Intelligence Accelerator and was accomplished under Cooperative Agreement Number FA8750-19-2-1000. The views and conclusions contained in this document are those of the authors and should not be interpreted as representing the official policies, either expressed or implied, of the United States Air Force or the U.S. Government. The U.S. Government is authorized to reproduce and distribute reprints for Government purposes, notwithstanding any copyright notation herein.

References

Advani, M. S., Saxe, A. M., and Sompolinsky, H. High-dimensional dynamics of generalization error in neural

- networks. *Neural Networks*, 132:428–446, 2020.
- Akemann, G., Ipsen, J. R., and Kieburg, M. Products of rectangular random matrices: singular values and progressive scattering. *Physical Review E*, 88(5):052118, 2013a.
- Akemann, G., Kieburg, M., and Wei, L. Singular value correlation functions for products of wishart random matrices. *Journal of Physics A: Mathematical and Theoretical*, 46(27):275205, 2013b.
- Arora, S., Cohen, N., and Hazan, E. On the optimization of deep networks: Implicit acceleration by overparameterization. In *ICML*, 2018.
- Arora, S., Cohen, N., Hu, W., and Luo, Y. Implicit regularization in deep matrix factorization. *Advances in Neural Information Processing Systems*, 32, 2019.
- Arpit, D., Jastrz̄ebski, S., Ballas, N., Krueger, D., Bengio, E., Kanwal, M. S., Maharaj, T., Fischer, A., Courville, A., Bengio, Y., et al. A closer look at memorization in deep networks. In *International Conference on Machine Learning*, pp. 233–242. PMLR, 2017.
- Belkin, M., Hsu, D., Ma, S., and Mandal, S. Reconciling modern machine-learning practice and the classical bias–variance trade-off. *Proceedings of the National Academy of Sciences*, 116(32):15849–15854, 2019.
- Bell-Kligler, S., Shocher, A., and Irani, M. Blind super-resolution kernel estimation using an internal-gan. In *Advances in Neural Information Processing Systems*, 2019.
- Burda, Z., Jarosz, A., Livan, G., Nowak, M. A., and Swiech, A. Eigenvalues and singular values of products of rectangular gaussian random matrices. *Physical Review E*, 82(6):061114, 2010.
- Dosovitskiy, A., Beyer, L., Kolesnikov, A., Weissenborn, D., Zhai, X., Unterthiner, T., Dehghani, M., Minderer, M., Heigold, G., Gelly, S., et al. An image is worth 16x16 words: Transformers for image recognition at scale. *arXiv preprint arXiv:2010.11929*, 2020.
- Eldan, R. and Shamir, O. The power of depth for feedforward neural networks. In *Conference on learning theory*, pp. 907–940. PMLR, 2016.
- Friedberg, S., Insel, A., and Spence, L. *Linear Algebra*. Featured Titles for Linear Algebra (Advanced) Series. Pearson Education, 2003. ISBN 9780130084514. URL <https://books.google.com/books?id=HCULAQAAIAAJ>.
- Geman, S., Bienenstock, E., and Doursat, R. Neural networks and the bias/variance dilemma. *Neural computation*, 4(1):1–58, 1992.

- Gidel, G., Bach, F., and Lacoste-Julien, S. Implicit regularization of discrete gradient dynamics in linear neural networks. In *Advances in Neural Information Processing Systems*, pp. 3202–3211, 2019.
- Golubeva, A., Neyshabur, B., and Gur-Ari, G. Are wider nets better given the same number of parameters? In *International Conference on Learning Representations*, 2021.
- Goodfellow, I. J., Vinyals, O., and Saxe, A. M. Qualitatively characterizing neural network optimization problems. In *International Conference on Learning Representations*, 2015.
- Gunasekar, S., Woodworth, B. E., Bhojanapalli, S., Neyshabur, B., and Srebro, N. Implicit regularization in matrix factorization. In *Advances in Neural Information Processing Systems*, pp. 6151–6159, 2017.
- Gunasekar, S., Lee, J. D., Soudry, D., and Srebro, N. Implicit bias of gradient descent on linear convolutional networks. In *Advances in Neural Information Processing Systems*, pp. 9461–9471, 2018.
- Guo, S., Alvarez, J. M., and Salzmann, M. Expandnets: Linear over-parameterization to train compact convolutional networks. In *Advances in Neural Information Processing Systems*, 2020.
- He, K., Zhang, X., Ren, S., and Sun, J. Deep residual learning for image recognition. In *Proceedings of the IEEE conference on computer vision and pattern recognition*, pp. 770–778, 2016.
- Hestness, J., Narang, S., Ardalani, N., Diamos, G., Jun, H., Kianinejad, H., Patwary, M., Ali, M., Yang, Y., and Zhou, Y. Deep learning scaling is predictable, empirically. *arXiv preprint arXiv:1712.00409*, 2017.
- Hoyer, S., Sohl-Dickstein, J., and Greydanus, S. Neural reparameterization improves structural optimization. *arXiv preprint arXiv:1909.04240*, 2019.
- Ioffe, S. and Szegedy, C. Batch normalization: Accelerating deep network training by reducing internal covariate shift. In *International conference on machine learning*, pp. 448–456. PMLR, 2015.
- Jacot, A., Gabriel, F., and Hongler, C. Neural tangent kernel: convergence and generalization in neural networks. In *Advances in Neural Information Processing Systems*, pp. 8580–8589, 2018.
- Jing, L., Zbontar, J., et al. Implicit rank-minimizing autoencoder. In *Advances in Neural Information Processing Systems*, volume 33, 2020.
- Kaplan, J., McCandlish, S., Henighan, T., Brown, T. B., Chess, B., Child, R., Gray, S., Radford, A., Wu, J., and Amodei, D. Scaling laws for neural language models. *arXiv preprint arXiv:2001.08361*, 2020.
- Kiros, R., Zhu, Y., Salakhutdinov, R., Zemel, R. S., Torralba, A., Urtasun, R., and Fidler, S. Skip-thought vectors. In *Advances in Neural Information Processing Systems*, 2015.
- Kriegeskorte, N., Mur, M., and Bandettini, P. Representational similarity analysis - connecting the branches of systems neuroscience. *Frontiers in Systems Neuroscience*, 2:4, 2008. ISSN 1662-5137. doi: 10.3389/neuro.06.004.2008. URL <https://www.frontiersin.org/article/10.3389/neuro.06.004.2008>.
- Krizhevsky, A., Hinton, G., et al. Learning multiple layers of features from tiny images. 2009.
- Krizhevsky, A., Sutskever, I., and Hinton, G. E. Imagenet classification with deep convolutional neural networks. *Advances in neural information processing systems*, 25: 1097–1105, 2012.
- Krizhevsky, A., Sutskever, I., and Hinton, G. E. Imagenet classification with deep convolutional neural networks. *Communications of the ACM*, 60(6):84–90, 2017.
- Li, Y., Ma, T., and Zhang, H. Algorithmic regularization in over-parameterized matrix sensing and neural networks with quadratic activations. In *Conference On Learning Theory*, pp. 2–47. PMLR, 2018.
- Ma, C., Wang, K., Chi, Y., and Chen, Y. Implicit regularization in nonconvex statistical estimation: Gradient descent converges linearly for phase retrieval and matrix completion. In *International Conference on Machine Learning*, pp. 3345–3354. PMLR, 2018.
- Mises, R. and Pollaczek-Geiringer, H. Praktische verfahren der gleichungsauflösung. *ZAMM-Journal of Applied Mathematics and Mechanics/Zeitschrift für Angewandte Mathematik und Mechanik*, 9(1):58–77, 1929.
- Nacson, M. S., Lee, J., Gunasekar, S., Savarese, P. H. P., Srebro, N., and Soudry, D. Convergence of gradient descent on separable data. In *The 22nd International Conference on Artificial Intelligence and Statistics*, pp. 3420–3428. PMLR, 2019.
- Nakkiran, P., Kaplun, G., Kalimeris, D., Yang, T., Edelman, B. L., Zhang, F., and Barak, B. Sgd on neural networks learns functions of increasing complexity. *arXiv preprint arXiv:1905.11604*, 2019.

- Neuschel, T. Plancherel–rotach formulae for average characteristic polynomials of products of ginibre random matrices and the fuss–catalan distribution. *Random Matrices: Theory and Applications*, 3(01):1450003, 2014.
- Neyshabur, B., Tomioka, R., and Srebro, N. In search of the real inductive bias: On the role of implicit regularization in deep learning. In *International conference on machine learning*, 2015.
- Nichani, E., Radhakrishnan, A., and Uhler, C. Do deeper convolutional networks perform better? *arXiv preprint arXiv:2010.09610*, 2020.
- Paszke, A., Gross, S., Massa, F., Lerer, A., Bradbury, J., Chanan, G., Killeen, T., Lin, Z., Gimelshein, N., Antiga, L., Desmaison, A., Kopf, A., Yang, E., DeVito, Z., Raison, M., Tejani, A., Chilamkurthy, S., Steiner, B., Fang, L., Bai, J., and Chintala, S. Pytorch: An imperative style, high-performance deep learning library. In Wallach, H., Larochelle, H., Beygelzimer, A., d’Alché-Buc, F., Fox, E., and Garnett, R. (eds.), *Advances in Neural Information Processing Systems 32*, pp. 8024–8035. Curran Associates, Inc., 2019. URL <http://papers.neurips.cc/paper/9015-pytorch-an-imperative-style-high-performance-deep-learning-library.pdf>.
- Pennington, J., Schoenholz, S. S., and Ganguli, S. Resurrecting the sigmoid in deep learning through dynamical isometry: theory and practice. In *Advances in neural information processing systems*, 2017.
- Pennington, J., Schoenholz, S., and Ganguli, S. The emergence of spectral universality in deep networks. In *International Conference on Artificial Intelligence and Statistics*, pp. 1924–1932. PMLR, 2018.
- Razin, N. and Cohen, N. Implicit regularization in deep learning may not be explainable by norms. In *Advances in neural information processing systems*, 2020.
- Rokach, L. and Maimon, O. Clustering methods. In *Data mining and knowledge discovery handbook*, pp. 321–352. Springer, 2005.
- Roy, O. and Vetterli, M. The effective rank: A measure of effective dimensionality. In *2007 15th European Signal Processing Conference*, pp. 606–610. IEEE, 2007.
- Russakovsky, O., Deng, J., Su, H., Krause, J., Satheesh, S., Ma, S., Huang, Z., Karpathy, A., Khosla, A., Bernstein, M., et al. Imagenet large scale visual recognition challenge. *International journal of computer vision*, 2015.
- Savitzky, A. and Golay, M. J. Smoothing and differentiation of data by simplified least squares procedures. *Analytical chemistry*, 36(8):1627–1639, 1964.
- Saxe, A. M., McClelland, J. L., and Ganguli, S. Exact solutions to the nonlinear dynamics of learning in deep linear neural network. In *In International Conference on Learning Representations*. Citeseer, 2014.
- Shah, H., Tamuly, K., Raghunathan, A., Jain, P., and Netrapalli, P. The pitfalls of simplicity bias in neural networks. *arXiv preprint arXiv:2006.07710*, 2020.
- Shah, V., Kyrillidis, A., and Sanghavi, S. Minimum norm solutions do not always generalize well for over-parameterized problems. In *stat*, volume 1050, pp. 16, 2018.
- Solomonoff, R. J. A formal theory of inductive inference. part i. *Information and control*, 7(1):1–22, 1964.
- Soudry, D., Hoffer, E., Nacson, M. S., Gunasekar, S., and Srebro, N. The implicit bias of gradient descent on separable data. *The Journal of Machine Learning Research*, 19(1):2822–2878, 2018.
- Szegedy, C., Liu, W., Jia, Y., Sermanet, P., Reed, S., Anguelov, D., Erhan, D., Vanhoucke, V., and Rabinovich, A. Going deeper with convolutions. In *Proceedings of the IEEE conference on computer vision and pattern recognition*, pp. 1–9, 2015.
- Tu, S., Boczar, R., Simchowitz, M., Soltanolkotabi, M., and Recht, B. Low-rank solutions of linear matrix equations via procrustes flow. In *International Conference on Machine Learning*, pp. 964–973. PMLR, 2016.
- Valle-Perez, G., Camargo, C. Q., and Louis, A. A. Deep learning generalizes because the parameter-function map is biased towards simple functions. In *International Conference on Learning Representations*, 2019.
- Vershynin, R. *High-dimensional probability: An introduction with applications in data science*, volume 47. Cambridge university press, 2018.
- Xie, S., Girshick, R., Dollár, P., Tu, Z., and He, K. Aggregated residual transformations for deep neural networks. In *Proceedings of the IEEE conference on computer vision and pattern recognition*, pp. 1492–1500, 2017.
- Yoshida, Y. and Miyato, T. Spectral norm regularization for improving the generalizability of deep learning. *arXiv preprint arXiv:1705.10941*, 2017.
- Zhang, C., Bengio, S., Hardt, M., Recht, B., and Vinyals, O. Understanding deep learning requires rethinking generalization. In *International Conference on Learning Representations*, 2017.
- Zhang, R., Isola, P., Efros, A. A., Shechtman, E., and Wang, O. The unreasonable effectiveness of deep features as a

perceptual metric. In *Proceedings of the IEEE conference on computer vision and pattern recognition*, 2018.

Zoph, B. and Le, Q. V. Neural architecture search with reinforcement learning. In *International Conference on Learning Representations*, 2017.

A. Comparisons of rank measures

The rank of a matrix – which defines the number of independent basis – can often be itself a sub-optimal measure. For deep learning, fluctuations in stochastic gradient descent and numerical imprecision can easily introduce noise that causes a matrix to be full-rank. In addition, simply counting the number of non-zero singular values may not be indicative of what we care about in practice: the relative impact of the i -th basis compared to the j -th basis. Effective rank was proposed to deal with these problems, and we have extensively used them throughout our work.

Definition 2 (Effective rank). (*Roy & Vetterli, 2007*)

For any matrix $A \in \mathbb{R}^{m \times n}$, the effective rank ρ is defined as the Shannon entropy of the normalized singular values:

$$\rho(A) = - \sum_{i=1}^{\min(n,m)} \bar{\sigma}_i \log(\bar{\sigma}_i),$$

where $\bar{\sigma}_i = \sigma_i / \sum_j \sigma_j$ are the normalized singular values such that $\sum_i \bar{\sigma}_i = 1$. It follows that $\rho(A) \leq \text{rank}(A)$. This measure is also known as the spectral entropy.

We now state other various metrics that have been used as a pseudo-measure of matrix rank. One obvious alternative is to use the original definition of rank after normalization:

Definition 3 (Threshold rank). For any matrix $A \in \mathbb{R}^{m \times n}$, the threshold rank τ -Rank is the count of non-small singular values after normalization:

$$\tau\text{-Rank}(A) = \sum_{i=1}^{\min(n,m)} \mathbb{1}[\bar{\sigma}_i \geq \tau],$$

where $\mathbb{1}$ is the indicator function, and $\tau \in [0, 1]$ is the threshold value. $\bar{\sigma}_i$ are the normalized singular values defined above.

It is worth noting that not normalizing the singular values results in the numerical definition of rank. Although the threshold rank is the closest to the original definition of rank, depending on the threshold value, a drastically different scalar representation of rank can emerge. Potentially, better usage of threshold rank is to measure the AUC when varying the threshold.

Related to the definition of the threshold rank, stable rank operates on the normalized squared-singular values:

Definition 4 (Stable rank). (*Vershynin, 2018*)

For any matrix, $A \in \mathbb{R}^{m \times n}$, the stable rank is defined as:

$$S\text{Rank}(A) = \frac{\|A\|_F^2}{\|A\|_2} = \frac{\sum \sigma_i^2}{\sigma_{\max}^2},$$

Where σ_i are the singular values of A .

Stable-rank provides the benefit of being efficient to approximate via the power iteration (*Mises & Pollaczek-Geiringer, 1929*). In general, stable-rank is a good proxy for measuring the rank of the matrix. This is not necessarily true when the singular values have a long tail distribution, which under-emphasizes the small singular values un-proportionately due to the squared-operator.

Lastly, the nuclear norm has been considered as the de facto measure of rank in the matrix factorization/completion community, with low nuclear-norm indicating that the matrix is low-rank:

Definition 5 (Nuclear norm). For any matrix $A \in \mathbb{R}^{m \times n}$, the nuclear norm operator is defined as:

$$\|A\|_* = \text{tr}(\sqrt{AA^T}) = \sum_i^{\min(n,m)} \sigma_i(A)$$

Where σ_i are the singular values of A .

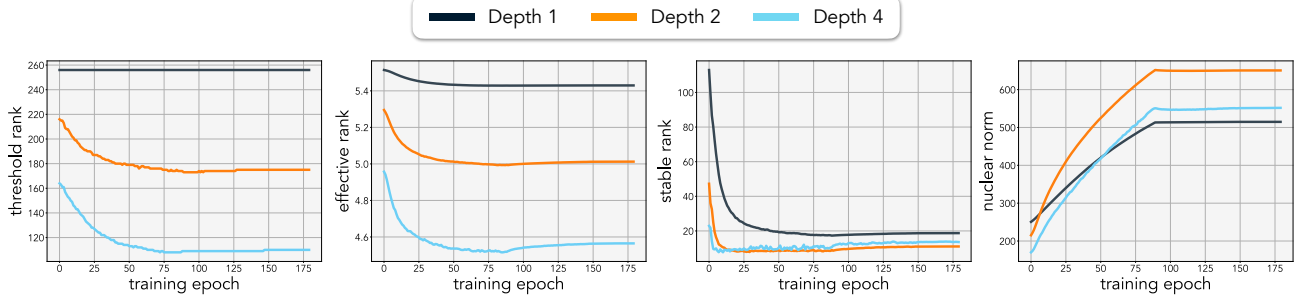


Figure 9. Comparing rank-measures: Comparison between various pseudo-metrics of rank when varying the number of layers. The threshold is set to $\tau = 0.01$ for threshold rank.

Nuclear norm, however, has obvious flaws of being an un-normalized measure. The nuclear norm is dictated by the magnitude of the singular values and not the ratios. Therefore, the nuclear norm can be made arbitrarily large or small without changing the output distribution.

The comparisons of these metrics are illustrated in Figure 9. The metrics are computed on the end-to-end weights throughout the training. We use linear over-parameterized models with various depths on least-squares.

B. Training details and model architecture

All models for image classification are trained using PyTorch (Paszke et al., 2019) with RTX 2080Ti GPUs. We use stochastic gradient descent with a momentum of 0.9. For CIFAR experiments, the initial learning rate is individually tuned (0.02 for most cases), and we train the model for 180 epochs. We use a step learning rate scheduler at epoch 90 and 150, decreasing the learning rate by a factor of 10 each step. For all the models, we use random-horizontal-flip and random-resize-crop for data augmentation. The training details for ImageNet can be found in <https://github.com/pytorch/examples/blob/master/imagenet>. We found it very important to re-tune the weight decay for larger models on ImageNet. The architecture used for the CIFAR experiments is:

CIFAR architecture	
RGB image $y \in \mathbb{R}^{32 \times 32 \times 3}$	
Convolution 3 \rightarrow 64, MaxPool, ReLU	
Convolution 64 \rightarrow 128, MaxPool, ReLU	
Convolution 128 \rightarrow 256, MaxPool, ReLU	
Convolution 256 \rightarrow 512, ReLU	
GlobalMaxPool	
Fully-Connected 512 \rightarrow 256, ReLU	
Fully-Connected 256 \rightarrow num classes	

C. Differential effective rank

To analyze the effective rank as a function of the number of layers, we define a differential variant of the effective rank. This formulation allows us to use the fact that the eigen/singular-value spectrum assumes a probability distribution in the asymptotic case.

Definition 6 (Differential effective rank). *For any matrix $A \in \mathbb{R}^{m \times n}$ as $\min(m, n) \rightarrow \infty$ the singular values assume a probability distribution $p(\sigma)$. Then, we define the differential effective rank ρ as:*

$$\rho(A) = - \int_{\sigma} \frac{\sigma}{c} \log\left(\frac{\sigma}{c}\right) p(\sigma) d\sigma \quad (3)$$

where $p(\sigma)$ is the singular value density function and $c = \int \sigma p(\sigma) d\sigma$ is the normalization constant.

D. Proof of Theorem 1

To prove Theorem 1, we leverage the findings from random matrix theory, where the singular values assumes a probability density function. Specifically, we use the density function corresponding to the singular values of matrix W composed of the product of L individual matrices $W = W_L \dots W_1$, where the components of the matrices W_1 to W_L are drawn i.i.d from a Gaussian. Characterizing such density function is in general intractable, or otherwise very difficult. However, in the asymptotic case where $\dim(W) \rightarrow \infty$ and W is square, the density function admits the following concise closed form (Eq. 13 of Pennington et al. (2017) derived from Neuschel (2014)):

$$p(\sigma(\phi)) = \frac{2}{\pi} \sqrt{\frac{\sin^3(\phi) \sin^{L-2}(L\phi)}{\sin^{L-1}((L+1)\phi)}} \quad \sigma(\phi) = \sqrt{\frac{\sin^{L+1}((L+1)\phi)}{\sin(\phi) \sin^L(L\phi)}}, \quad (4)$$

where σ denotes singular values (parameterized by $\phi \in [0, \frac{\pi}{L+1}]$) and p denotes the probability density function of σ for $\sigma \in [0, \sigma_{\max}]$, and $\sigma_{\max}^2 = L^{-L}(L+1)^{L+1}$. The parametric probability density function spans the whole singular value spectrum when sweeping the variable ϕ .

We are interested in computing effective rank of W . Using the above density function, we can write it in the form:

$$\rho(W) = - \int_0^{\sigma_{\max}} \frac{\sigma}{c} \log\left(\frac{\sigma}{c}\right) p(\sigma) d\sigma, \quad (5)$$

We now write this integral in terms of ϕ as the integration variable, such that we can leverage the density function in Eqn. 4. Using the change of variable we have:

$$\rho(W; L) = - \int_0^{\frac{\pi}{L+1}} \frac{\sigma(\phi)}{c} \log\left(\frac{\sigma(\phi)}{c}\right) (-p(\sigma(\phi))\sigma'(\phi)) d\phi, \quad (6)$$

where $\sigma'(\phi) = \frac{d}{d\phi}\sigma(\phi)$. Note that the integral limits $[0, \sigma_{\max}]$ on σ respectively translate³ into $[\frac{\pi}{L+1}, 0]$ on ϕ . Computing the inner probability term, we get:

$$-p(\sigma(\phi))\sigma'(\phi) = \frac{1}{2\pi} \left(1 + L + L^2 - L(L+1) \cos(2\phi) - (L+1) \cos(2L\phi) + L \cos(2(1+L)\phi) \right) \csc^2(L\phi).$$

As $\rho(W; L)$ is differentiable in L , $\rho(W; L)$ decreases in L if and only if $\frac{d\rho}{dL} < 0$. Since integration and differentiation are w.r.t. different variables, they commute; we can first compute the derivative of the integrand w.r.t. L and then integrate w.r.t. ϕ and show that the result is negative.

The integrand can be expressed as:

$$-\frac{\sigma(\phi)}{c} \log\left(\frac{\sigma(\phi)}{c}\right) (-p(\sigma(\phi))\sigma'(\phi)) = hv^2 \log(u) \sqrt{u}, \quad (7)$$

³note that the direction of integration needs to flip (by multiplying by -1) to account for flip of the upper and lower limits.

where the variables h , v and u are defined as:

$$h = \frac{1}{4\pi} \left(1 + L(L+1)(1 - \cos(2\phi)) - (1+L) \cos(2L\phi) + L \cos(2(1+L)\phi) \right) \quad (8)$$

$$v = \csc(L\phi)$$

$$u = \frac{L^L}{(L+1)^{L+1}} \csc(\phi) \sin^{-L}(L\phi) \sin^{L+1}((L+1)\phi). \quad (9)$$

Now it is straightforward to differentiate the integrand and show that it has the following form:

$$\frac{d}{dL} hv^2 \log(u) \sqrt{u} = \frac{v(h(2 + \log(u))vu' + 2\log(u)u(vh' + 2hv'))}{2\sqrt{u}} \quad (10)$$

We should now integrate the above form w.r.t. ϕ from 0 to $\frac{\pi}{L+1}$ and examine the sign of the integrated form. The Eqn. 10 is positive for smaller ϕ and negative for larger ϕ . Furthermore, the area under the positive region is smaller than the negative one; hence, the total value of the integral is negative. This completes the proof that the singular values decrease as a function of the number of layers.

The proof here considers the asymptotic case when $\dim(W) \rightarrow \infty$. This limit case allowed us to use the probability distribution of the singular values. Although we do not provide proof for the finite-case, our results demonstrates that it holds empirically in practice (see Figure 2).

E. Least-squares learning dynamics

The learning dynamics of a linear network change when over-parameterized. Here, we derive the effective update rule on least-squares using linear neural networks to provide motivation on why they have differing update dynamics. For a single-layer linear network parameterized by W , without bias, the update rule is:

$$W^{(t+1)} \leftarrow W^{(t)} - \eta \nabla_{W^{(t)}} \mathcal{L}(W^{(t)}, x, y) \quad (11)$$

$$= W^{(t)} - \eta \nabla_{W^{(t)}} \frac{1}{2} (y - W^{(t)}x)^2 \quad (12)$$

$$= W^{(t)} - \eta (W^{(t)}xx^T - yx^T) \quad (13)$$

Where η is the the learning rate. Similarly, the update rule for the two-layer network $y = W_e x = W_2 W_1 x$ can be written as:

$$W_1^{(t+1)} \leftarrow W_1^{(t)} - \eta (W_2^{(t)})^T (W_e^{(t)}xx^T - yx^T) \quad (14)$$

$$W_2^{(t+1)} \leftarrow W_2^{(t)} - \eta (W_e^{(t)}xx^T - yx^T) (W_1^{(t)})^T \quad (15)$$

$$(16)$$

Using a short hand notation for $\nabla \mathcal{L}^{(t)} = W_e^{(t)}xx^T - yx^T$, we can compute the effective update rule for the two-layer network:

$$W_e^{(t+1)} = W_2^{(t+1)} W_1^{(t+1)} \quad (17)$$

$$= (W_2^{(t)} - \eta \nabla \mathcal{L}^{(t)} W_1^{(t)T}) (W_1^{(t)} - \eta W_2^{(t)T} \nabla \mathcal{L}^{(t)}) \quad (18)$$

$$= W_2^{(t)} W_1^{(t)} - \eta W_2^{(t)} W_2^{(t)T} \nabla \mathcal{L}^{(t)} - \eta \nabla \mathcal{L}^{(t)} W_1^{(t)T} W_1^{(t)} + \eta^2 \nabla \mathcal{L}^{(t)} W_1^{(t)T} W_2^{(t)T} \nabla \mathcal{L}^{(t)} \quad (19)$$

$$= W_e^{(t)} - \underbrace{\eta (W_2^{(t)} W_2^{(t)T} \nabla \mathcal{L}^{(t)} + \nabla \mathcal{L}^{(t)} W_1^{(t)T} W_1^{(t)})}_{\text{first order } \mathcal{O}(\eta)} + \underbrace{\eta^2 \nabla \mathcal{L}^{(t)} W_1^{(t)T} W_2^{(t)T} \nabla \mathcal{L}^{(t)}}_{\text{second order } \mathcal{O}(\eta^2)} \quad (20)$$

$$\approx W_e^{(t)} - \eta (P_2 \nabla \mathcal{L}^{(t)} + \nabla \mathcal{L}^{(t)} P_1^T) \quad (21)$$

Where $P_i^{(t)} = W_i^{(t)}W_i^{(t)T}$ are the preconditioning matrices. The higher order terms can be ignored if the step-size is chosen sufficiently small.

(special-case 1) If the weight matrices are *orthonormal*, then the update rule is equivalent upto a scale to the original:

$$W_e^{(t+1)} = W_e^{(t)} - 2\eta \nabla \mathcal{L}^{(t)} + \eta^2 \nabla \mathcal{L}^{(t)} W_e^{(t)T} \nabla \mathcal{L}^{(t)} \quad (22)$$

$$\approx W_e^{(t)} - 2\eta \nabla \mathcal{L}^{(t)} \quad (23)$$

(special-case 2) If the weights are uncorrelated and $\dim(W) \gg 1$, then WW^T and W^TW are approximately diagonal. This implies the weights, in most cases, are only getting re-scaled.

$$\approx W_e^{(t)} - \eta(D_2 \nabla \mathcal{L}^{(t)} + \nabla \mathcal{L}^{(t)} D_1) \quad (24)$$

This condition is generally true at initialization for models that are randomly initialized from a Gaussian or uniform distribution. Whether this condition holds throughout training is unknown.

(general case) For a linear network with p -layer expansion, the update for layer $1 \leq i \leq p$ is:

$$W_i^{(t+1)} \leftarrow W_i^{(t)} - \eta \underbrace{(W_p^{(t)} \cdots W_{i+1}^{(t)})^T}_{\text{weights } > i} \underbrace{(\nabla \mathcal{L}^{(t)} W_e^{(t)} x x^T - y x^T)}_{\text{original gradient}} \underbrace{(W_{i-1}^{(t)} \cdots W_1^{(t)})^T}_{\text{weights } < i} \quad (25)$$

Denoting $W_{j:i} = W_j \cdots W_{i+1} W_i$ for $j > i$, the effective update rule for the end-to-end matrix is:

$$W_e^{(t+1)} = \prod_{1 < i < p} W_i^{(t+1)} = \prod_{1 < i < p} (W_i - \eta W_{p:i+1}^{(t)T} \nabla \mathcal{L}^{(t)} W_{i-1:1}^T) \quad (26)$$

$$= W_e^{(t)} - \eta \sum_{1 < i < p} W_{p:i+1} W_{p:i+1}^T \nabla \mathcal{L}^{(t)} W_{i-1:1}^T W_{i-1:1} + \mathcal{O}(\eta^2) + \cdots + \mathcal{O}(\eta^p) \quad (27)$$

$$\approx W_e^{(t)} - \eta \sum_{1 < i < p} \underbrace{W_{p:i+1} W_{p:i+1}^T}_{\text{left precondition}} \underbrace{\nabla \mathcal{L}^{(t)}}_{\text{original gradient}} \underbrace{W_{i-1:1}^T W_{i-1:1}}_{\text{right precondition}} \quad (28)$$

The update rule for general case has a much more complicated interaction of variables. For the edge $i = 1$ and $i = p$ the left and right preconditioning matrix is an identity matrix respectively. Similarly, special-case arguments can be applied here.

F. Kernel rank-landscape

We visualize the effective rank landscape of the kernels in Figure 10. We use two-layer and four-layer ReLU networks, where the weights are sampled from the same distribution. The kernels are constructed from 128 randomly sampled input data. The input data is fixed when moving along the random directions u, v . Similar to the linear network, we observe that over-parameterized non-linear models exhibit lower rank-landscape.

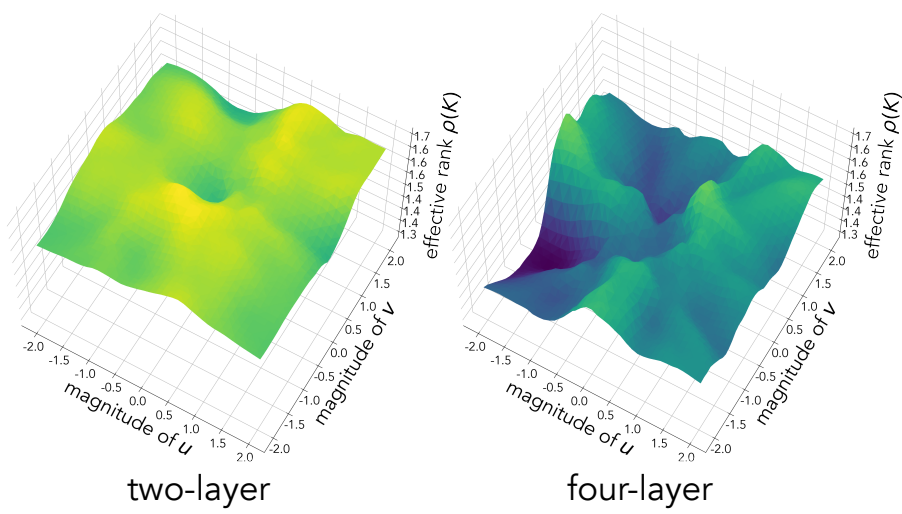


Figure 10. **Kernel rank landscape:** The landscape of the effective rank ρ computed on the kernels constructed from random features.